

Multimode vibration control of a smart model frame structure

Vineet Sethi¹ and Gangbing Song^{2,3}

¹ Department of Engineering Technology, University of Houston, 4800 Calhoun Road, Houston, TX 77204-4006, USA

² Department of Mechanical Engineering, University of Houston, 4800 Calhoun Road, Houston, TX 77204-4006, USA

E-mail: gsong@uh.edu

Received 23 September 2004, in final form 12 December 2005

Published 10 February 2006

Online at stacks.iop.org/SMS/15/473

Abstract

This paper investigates multimodal vibration control of a three-story model structural frame by using surface bonded PZT (lead zirconate titanate) type piezoceramic patches. Piezoceramic is one of the smart materials. Complete control systems design is synthesized on the model frame using system identification and a pole placement controller. A time domain based subspace system identification is performed to identify the first three modes of the structural frame. A fit of 90% is achieved in identification results. A full-state pole placement feedback controller is designed based on the identified model. To implement the full-state feedback controller, the design of a state estimator is also performed. Experimental results demonstrate the effectiveness of multimodal active control of the smart frame structure using pole placement control.

(Some figures in this article are in colour only in the electronic version)

1. Introduction

Protection of civil structures from dynamic loading under severe winds and earthquakes has attracted increasing attention in structural control worldwide. Traditionally, building structures have relied on their strength and ability to dissipate energy to survive under severe dynamic loading (Spencer and Sain 1997). Civil structural control has been investigated by means of active, passive, semi-active or hybrid vibration control methods. Soong (1988) reviewed the importance and necessity of active vibration control in civil engineering. Since this concept was non-traditional for civil engineering, real obstacles with respect to its acceptance existed at that time (Soong 1988). Active mass tuned dampers have been installed in buildings and TV towers (Cao *et al* 1998) and they have been successful because they can produce tons of forces necessary for the structural response control of the buildings. However, active/passive mass dampers have limitations too. They have high inherent costs and besides this the associated costs of the driving power source are also high (Valliappan and Qi 2001). To overcome the above limitations, the answer may lie in intelligent or smart structures.

³ Author to whom any correspondence should be addressed.

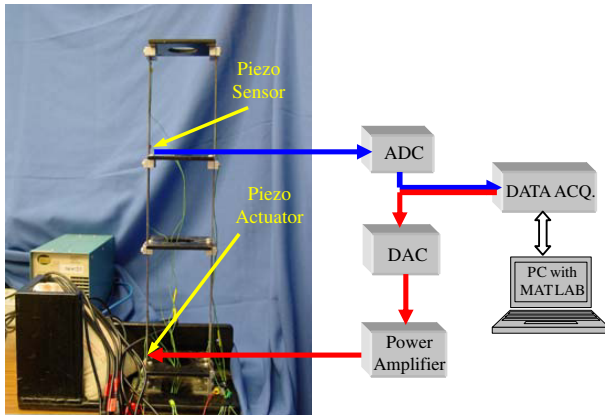
In recent years, smart structures have gained importance in vibration suppression primarily because of their advantages of being integrated with the structures. These structures facilitate the implementation of active vibration control. Not only can a parameter be identified easily in such structures but also various existing control strategies can be implemented for either single or multimodal vibration suppression. Piezoceramic or lead zirconate titanate (PZT) smart materials have been predominantly considered for active vibration suppression (Bailey and Hubbard 1985, Lazarus and Crawley 1992, Hagood and Anderson 1992, Crawley 1994).

One of the simple but effective methods for multimodal active vibration suppression is pole placement control. In this control strategy, the designer has the flexibility to place the poles at the desired location to achieve desired performance. Pole placement control has been successfully implemented by Manning *et al* (2000), Scott *et al* (2001) and Bu *et al* (2003) for control of the first dominant mode of flexible beams.

This investigation uses piezoceramic smart materials as actuator and sensor for multimodal active vibration control of a model frame structure. Control design of flexible structures relies on accurate modeling of the system dynamics, in the absence of adaptive or robust control (Saunders *et al* 1994).

Table 1. PZT-5H patch properties.

Symbol	Quantity	PZT actuator	PZT sensor
$L \times w \times t$	Dimensions	$70 \times 30 \times 0.25 \text{ mm}^3$	$15 \times 12 \times 0.25 \text{ mm}^3$
d_{33}	Strain coefficient	$5.93 \times 10^{-10} \text{ C N}^{-1}$	$5.93 \times 10^{-10} \text{ C N}^{-1}$
d_{31}	Strain coefficient	$-2.74 \times 10^{-10} \text{ C N}^{-1}$	$-2.74 \times 10^{-10} \text{ C N}^{-1}$
ρ_p	PZT density	7500 kg m^{-3}	7500 kg m^{-3}
E_p	Young's modulus	$6.3 \times 10^{10} \text{ N m}^{-2}$	$6.3 \times 10^{10} \text{ N m}^{-2}$

**Figure 1.** Experimental set-up.

In this paper, since it is multimodal control and a single sensor and actuator is used, the control strategy depends on the system identification and state estimator for the building structure. Several system identification models and their theory have been developed in (Ljung 1999) and are well adapted to structural system identification. Ghanem and Shinozuka (1995) reviewed system identification methods and their applications to earthquake engineering.

As the civil engineering embraces lighter and flexible structures the need to implement simultaneous multimodal control increases because it is insufficient to just control the first dominant mode of the structure. Some related multimodal control research was published by (Fujita *et al* 1993, Kar *et al* 2000, Rew *et al* 2002). Building or frame structure control has been investigated by Kamada *et al* (1997) and Aizawa *et al* (1998) and Fujita *et al* (2001).

To analyze the problem considered, investigative research is performed on a model structural frame which is described in the experimental set-up section. An approach for the controller synthesis is presented in this paper that first reviews some established concepts about system identification and presents the results of an experimental parametric state space model of the building. Based on the parametric model, a pole placement controller with a state estimator is designed. Finally, experimental results from pole placement control and the state estimator are presented.

2. Experimental set-up

The control objective is to optimally suppress the vibrations of a three-floor model building by using smart sensors and actuators. The set-up is shown in figure 1 and the dimensions are listed in table 1. Two larger PZT-5H patches are surface-bonded on either side of the support beam near its base end.

Table 2. Model building dimensions.

Symbol	Quantity	Units	Value
L	Length	mm	535
w_b	Width	mm	108
t	Thickness	mm	30
t_b	Thickness of the beam	mm	2

These PZT patches are used as actuators to excite the building and to enable active control of the model building vibration. There is also one PZT patch, surface bonded at the bottom of the third floor, which acts as a sensor. The sensor provides the feedback signal in the active control algorithm. The properties of PZT are shown in table 2. In this experiment, there is one input for the two actuators and one output was recorded from the sensor.

For implementing the controller in real time, a dSPACE digital data acquisition and real-time control system is used. The dSPACE uses a DS1103 digital signal process board for real-time control implementations. The dSPACE system also has integrated analog-to-digital and digital-to-analog converters.

3. System identification

3.1. Theoretical concepts

The approach of determining the transfer function using mathematical modeling and finite element analysis is complex. The finite element models sometimes are not feasible for control purposes because the order of the system model is high for achieving the desired accuracy. However, a system identification technique based upon experimentation offers a rather simplistic approach for getting the transfer function of the system. Based upon the input the output signals from the system are analyzed in order to get a model.

In this paper, the system identification algorithm used to identify the system is based upon the subspace method. A linear system can be represented in the state space innovation form as

$$\begin{aligned} x(t+1) &= Ax(t) + Bu(t) + Ke(t) \\ y(t) &= Cx(t) + Du(t) + e(t) \end{aligned} \quad (1)$$

where $e(t)$ is the innovations, i.e. the output that cannot be predicted from the past data, $x(t)$ is the state vector, $y(t)$ is the output, $u(t)$ is the input and K is the Kalman gain.

The subspace method can be used to estimate the A , B , C , D and K matrices. Assuming that $x(t)$, $y(t)$ and $u(t)$ are known, equation (1) becomes a linear regression. This will enable us to estimate the matrices C and D by the least squares method and will lead us to determine $e(t)$. Again,

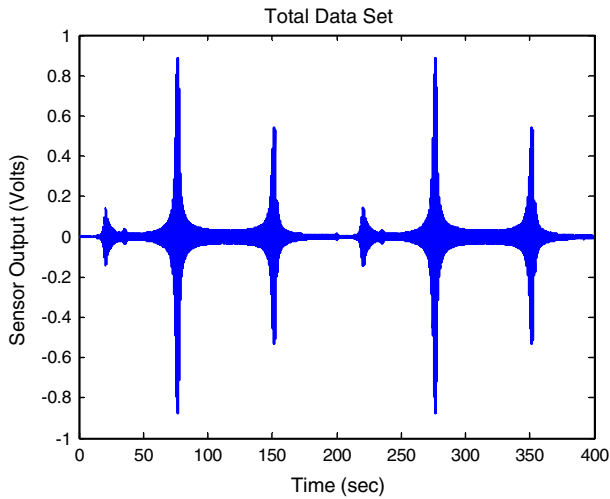


Figure 2. Evaluation and validation data set.

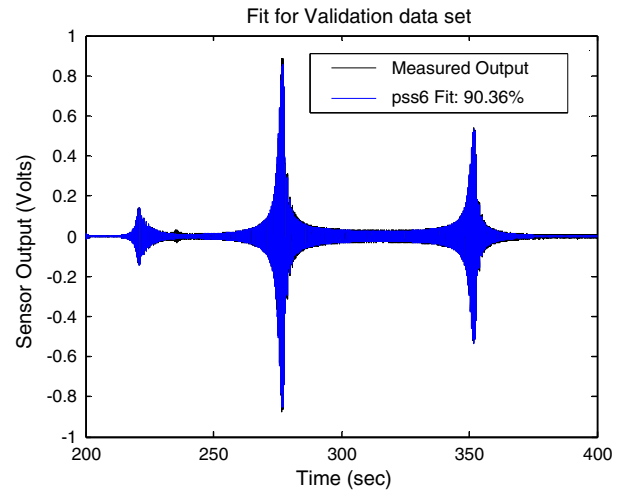


Figure 3. Identified model fit for validation data set.

$e(t)$ can be treated as known signal and this will lead us to determine A , B and K using the least squares method. The Kalman gain K is computed using the Riccati equation. In the above method, initially it is assumed that states $x(t)$ are known but they need to be determined. The states $x(t)$ can be formed as linear combinations of the k step ahead predicted outputs. The predictor, in this method, can be determined using the k step ahead predictors by projections from the observed data sequences. The above model derived from the subspace method is then used as a base model for further refining the model by the prediction error method (PEM).

In the time domain, the above system can be represented by using the shift operator q as

$$y(t) = G(q)u(t) + H(q)e(t) \quad (2)$$

$$G(q) = C(qI - A)^{-1}B + D \quad (3)$$

$$H(q) = C(qI - A)^{-1}K + I \quad (4)$$

where $G(q)$ is the transfer function of the system, $e(t)$ is the innovations, and I is the identity matrix.

From the observed data of input u and output y , the prediction errors can be computed as

$$e(t) = H^{-1}(q)[y(t) - G(q)u(t)]. \quad (5)$$

The above error can now be parametrized by the state space matrices derived above by the subspace method. A common parametric identification method is to determine estimates of G and H by minimizing

$$V_N(G, H) = \sum_{t=1}^N e^2(t). \quad (6)$$

This forms the basis for prediction error method. The model is first initialized and the further adjusted by optimizing the prediction error fit. Substantial details for system identification can be found in Ljung (1999) and the MATLAB (2002) toolbox reference manual. The prediction error method first initializes the model by using the subspace algorithm and then minimizes the prediction error.

Table 3. Frequency comparison.

	Experimental frequency (Hz)	Identified model frequency (Hz)
First mode	7.66	7.70
Second mode	23.89	24.03
Third mode	45.81	45.67

In this paper, a state space realization that does not model the noise properties, i.e. an output error model ($K = 0$), is considered. Thus, the implications will be on the predictors which will be based on the past inputs only.

3.2. Experimental identification results

Using the discussed experimental set-up, the piezo-actuators are excited by a sweep sinusoidal signal of frequency varying from 1 to 75 Hz in a sweep time of 200 s. The actuator signal is amplified using a power amplifier and the input voltage is set at 120 V. The samples are collected at a frequency of 250 Hz for 400 s so as to collect substantial data for model parametrization. The data collected are detrended and are used for evaluation and validation of the model. Figure 2 shows the output signal from the structure or the total data set collected for evaluation and validation by excitation of the structure using a sweep sine signal. Using the MATLAB System Identification toolbox a state space model of sixth order is obtained. Similar to the evaluation data, another experiment was performed to capture the validation data. Figure 3 shows the validation results of the identified model with a fit of 90%. This fit represents least squares error. Using the experimental data, the transfer function of the system can be found. The transfer function magnitude plot of the identified state space model is shown along with the experimental transfer function in figure 4. The identified model accurately captures the dynamics of the building structure. The frequency response in figure 4 of the identified model clearly shows the resonance frequencies at 7.70 Hz (48.4 rad s^{-1}), 24.03 Hz ($151.04 \text{ rad s}^{-1}$) and 45.67 Hz ($286.95 \text{ rad s}^{-1}$). Table 3 compares the experimental frequencies of the model building with that of the identified model.

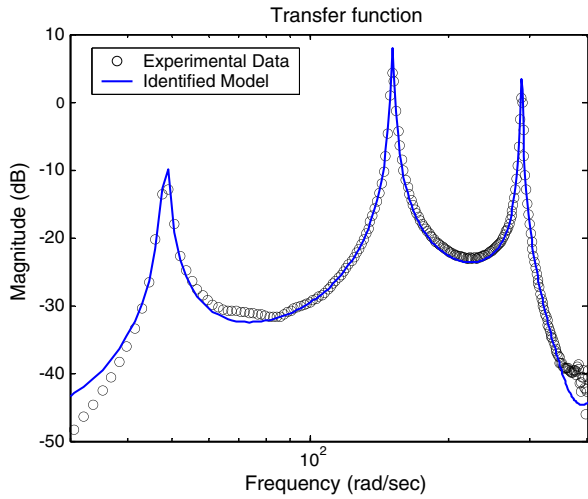


Figure 4. Frequency response of the identified model.

4. The pole placement controller and the state estimator

4.1. Design

The pole placement technique offers the designer the flexibility to select n independent gains in a system so that the arbitrarily assigned/desired pole performance is achieved. In this research, a linear pole placement controller is designed to control the first three modes of the flexible structure. A continuous time state space representation of the system is given by

$$\begin{aligned} \dot{x} &= Ax + Bu \\ y &= Cx + Du \end{aligned} \quad (7)$$

where the variables are given as follows. x : state variable vector. y : output in voltage. This is a weighted combination of state variable vectors. In this case it is the voltage output from the piezo-sensor. u : input vector; in this case it is the pre-amplified voltage to the piezo-actuator.

Once the matrix governing the state vector x is known, the feedback controller u can be determined by

$$u = -Kx \quad (8)$$

so as to achieve the desired performance of the closed loop system. Substituting the state feedback u in equation (7),

$$\begin{aligned} \dot{x} &= (A - BK)x \\ y &= (C - DK)x. \end{aligned} \quad (9)$$

The eigenvalues of matrix $(A - BK)$ determine the closed loop performance of the system. The feedback gain K is determined by the Ackermann's method. In our problem of vibration suppression, the requirement is to increase the damping of the system in order to quell the excessive vibrations. A necessary and sufficient condition for the pole placement problem is that the system has to be controllable. However, it is not practically possible to place the poles at arbitrary locations as the control effort may be too large for the actuators or large feedback gains may induce spill-over problems.

Table 4. Existing pole locations.

Existing pole	Frequency (rad s ⁻¹)	Damping ratio
$-0.26 \pm 48.4j$	48.4	0.0053
$-0.84 \pm 151.0j$	151	0.0055
$-1.03 \pm 287.0j$	287	0.0036

It is to be noted that in the above pole placement controller u the feedback is of the full states x of the system. However, in a practical situation we may not always be able to obtain the entire states of the system and often the output is a possible combination of all the states. In such situations we need a state estimator or observer to get full states of the system. The design of the state estimator is similar and can be done by the above pole assignment technique. The dynamics of the estimator is given by

$$\begin{aligned} \dot{\hat{x}} &= A\hat{x} + Bu + L(y - \hat{y}) \\ \hat{y} &= C\hat{x} + Du \end{aligned} \quad (10)$$

where L is the estimator gain that determines the convergence of $x \rightarrow \hat{x}$. The desired poles of the estimator are taken to be twice as fast as the desired poles of the closed loop system so as to ensure convergence. The estimator gain can be found by the conventional Ackermann formula by forming the dual of the system given by equation (7).

$$\dot{x} - \dot{\hat{x}} = Ax + Bu - A\hat{x} - Bu - L(y - \hat{y}). \quad (11)$$

Define $\varepsilon = x - \hat{x}$

$$\begin{aligned} \dot{\varepsilon} &= \dot{x} - \dot{\hat{x}} = A(x - \hat{x}) - L(Cx + Du - C\hat{x} - Du) \\ \dot{\varepsilon} &= (A - LC)\varepsilon. \end{aligned} \quad (12)$$

Thus, if we put observer in a closed loop system, the controller will be modified as

$$u = -K\hat{x}. \quad (13)$$

The closed loop system can be written as

$$\begin{aligned} \dot{x} &= Ax - BK\hat{x} = (A - BK)x + BK(x - \hat{x}) \\ \dot{\varepsilon} &= (A - LC)\varepsilon. \end{aligned} \quad (14)$$

In a matrix form, the above closed loop system is summarized as

$$\begin{bmatrix} \dot{x} \\ \dot{\varepsilon} \end{bmatrix} = \begin{bmatrix} (A - BK) & BK \\ 0 & (A - LC) \end{bmatrix} \begin{bmatrix} x \\ \varepsilon \end{bmatrix}. \quad (15)$$

The eigenvalues of the above matrix are the eigenvalues of $(A - BK)$ and the eigenvalues of $(A - LC)$. From above it is clear that we can choose the pole placement controller feedback gain K and observer gain L independently.

For effective vibration suppression it is necessary to choose closed loop poles appropriately. Table 4 lists the open loop poles of the continuous time reduced order system and the damping associated with it. Table 5 lists the desired closed loop poles and the desired damping. Evidently from tables 4 and 5 it is clear that we are increasing damping of the first three modes of the system. The desired poles when substituted in equation (9) will give the feedback gain K by Ackermann's

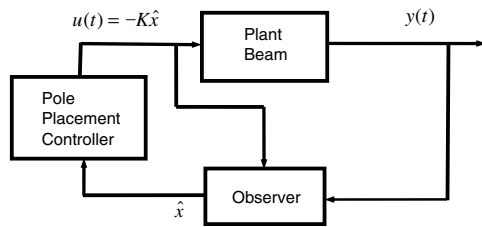


Figure 5. Closed loop system with observer.

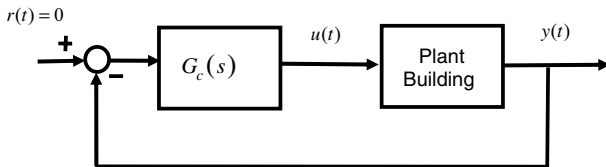


Figure 6. Block diagram of the system with observer controller.

Table 5. Desired pole locations.

Desired pole	Frequency (rad s ⁻¹)	Damping ratio
$-2.5 \pm 49.9j$	50	0.05
$-4.56 \pm 151.9j$	152	0.03
$-5.80 \pm 289.9j$	290	0.02

method. Thus, now we need to get the states of the system for the feedback law. These states can be obtained by the observer given in equation (10) for which we use the pole assignment approach. The poles of the observer are taken as twice the desired closed poles given in table 5. The observer gain L is found similarly by the pole assignment techniques and forming the dual of the given plant. Graphically, the closed loop system is shown in figure 5.

4.2. Transfer function of the controller

The block diagram shown in figure 5 can be simplified to that in figure 6, where the transfer function of the controller is in the frequency domain representation. The transfer function of the controller is given as

$$G_c(s) = K(sI - A + LC + BK)^{-1}L \quad (16)$$

where the variables are the same as defined earlier in section 4.1. Using equation (16), the frequency response of the observer controller is plotted in figure 7. Evidently, the designed observer controller is stable and rolls off at the high frequencies.

5. Experimental results of multimode vibration control

The identified model coupled with the pole placement controller is implemented in real time configuration. The model building is excited using three sinusoidal signals of modal frequencies for an initial 5 s at 40 V each, together with a noise input. The controller was implemented in a real time data

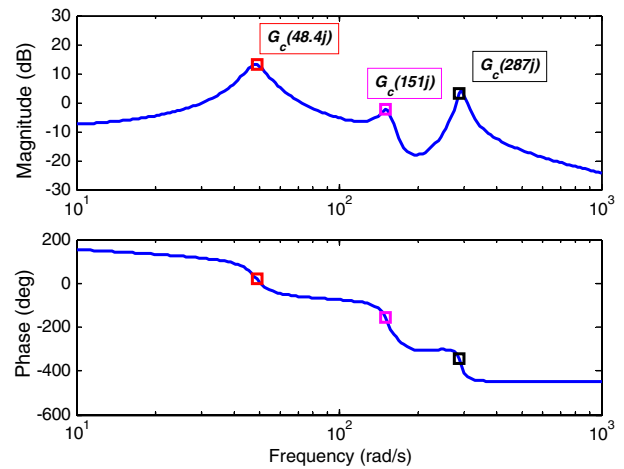


Figure 7. Frequency response of the observer controller.

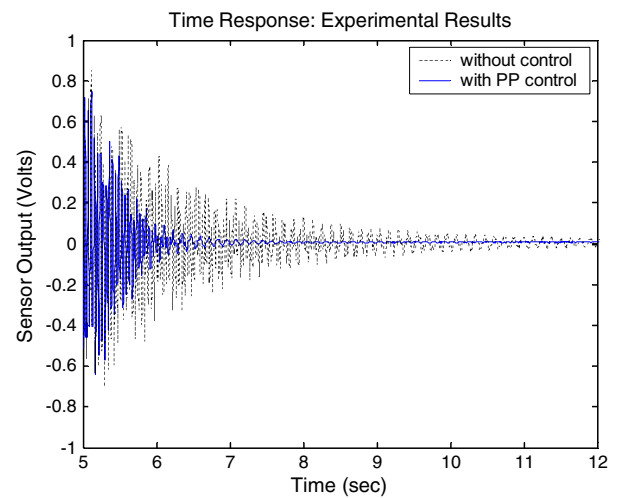


Figure 8. Comparative time response.

acquisition system with a sampling frequency of 1 kHz. The open loop test is conducted to view the results in the absence of the controller and the free vibration (without control) results are shown in figure 8. Next, the controller was implemented. The real time pole placement control time response is shown in figure 8. The uncontrolled vibrations that took about 7 s to die are now suppressed within 2 s. The power spectral density comparison plots for 6–12 s of the data are shown in figure 9. The power spectral density from 6 to 12 s is considered because the sudden kicking of control action after the excitation at 5 s might lead to excitation of higher modes, which die down because of their own damping over the next second. Evidently, substantial drops are observed simultaneously in the first three modes of the model building.

To implement the controller in real time, low pass and band pass filters are used. This is done to prevent the spill-over effects. The piezoelectric actuators have a tendency to excite the higher order modes more strongly than the other actuation mechanisms. Therefore, it becomes imperative to employ the filters. In the absence of filters, the spill-over effect was observed. The observer results in the free vibration

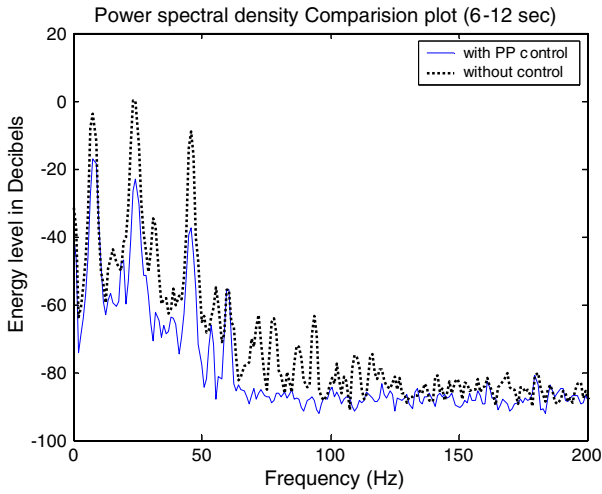


Figure 9. Comparative power spectral density plots.

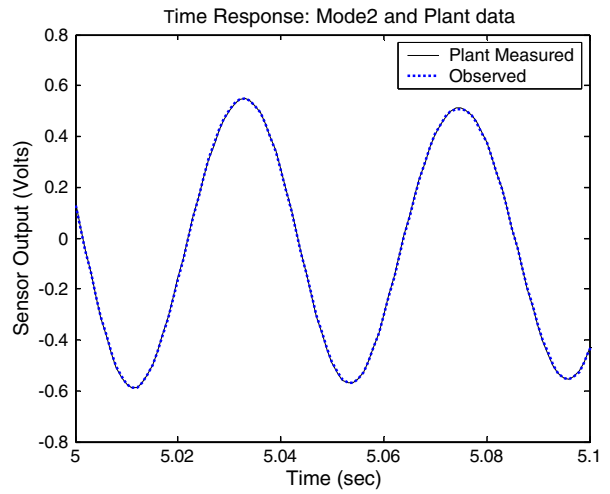


Figure 11. Comparative time response of second mode for measured and observed output in free vibration case.

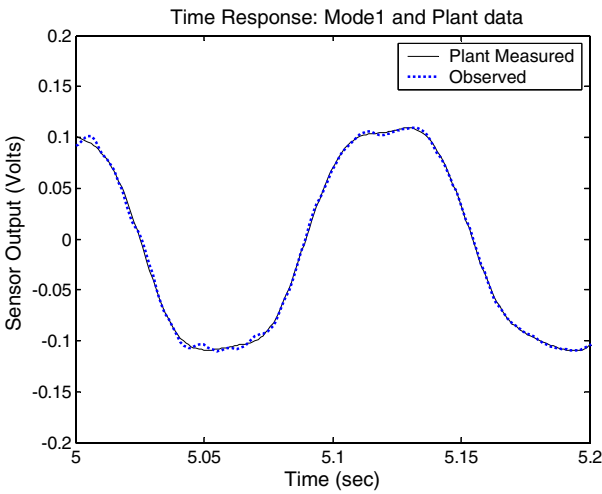


Figure 10. Comparative time response of first mode for measured and observed output in free vibration case.

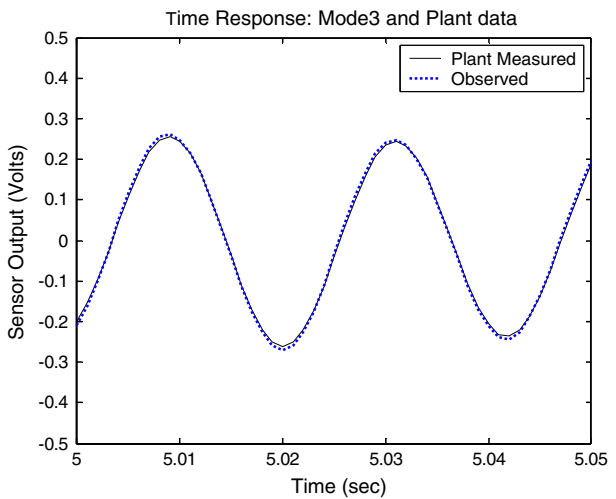


Figure 12. Comparative time response of third mode for measured and observed output in free vibration case.

case for the first three modes are also shown in figures 10, 11 and 12 respectively. From the figures it can be seen that the observer outputs closely match with the plant outputs for the respective modes. The plant outputs for the respective modes were acquired using band pass filters.

6. Discussions and conclusions

This paper presented investigative results on multimodal vibration control of building structures using piezoceramics. A control system design was presented which included parametric system identification, a full state pole placement controller and estimator for implementing full state feedback control. The parametric model with a 90% fit accurately represents the dynamics of the system as verified experimentally. The observer design gives the full states of the system accurately for use in feedback control design. The observer output for the respective modes confirms that the observer output converges to the true plant output in few tenths

of second. Finally, the pole placement control proves to be very effective in multimodal vibration suppression. The power spectrum density plot clearly demonstrates its effectiveness for multimode control.

It is anticipated that the above methodology is applicable to real life structures; however, there are certain issues in term of the control forces provided by piezoelectric patches that need to be investigated. Researchers have used piezoelectric stack actuators that provide large actuation forces for control of model building structures. In this regard Fujita *et al* (2002) tested a large scale piezoelectric stack actuator in their laboratory which provided a maximum force of 270 kN. They concluded that a smart structure with a large scale piezoelectric actuator could perform the same active control in stronger excitation than the hybrid mass damper could. Thus their research reinforces the point that we are not far from the time when these large scale piezoelectric actuators could be seen in action in large building structures.

Acknowledgments

The second author would like to thank the NSF for the support provided through grants 0305027 and 0341143 in conducting this research. Any opinions, findings and conclusions or recommendations expressed in this material are those of the author(s) and do not necessarily reflect the views of the sponsor.

References

- Aizawa S, Kakizawa T and Higasino M 1998 Case studies of smart materials for civil structures *Smart Mater. Struct.* **7** 617–26
- Bailey T and Hubbard E J Jr 1985 Distributed piezoelectric–polymer active vibration control of a cantilever beam *J. Guid. Control. Dyn.* **8** 605–11
- Bu X, Ye L, Su Z and Wang C 2003 Active control of a flexible smart beam using a system identification technique based on ARMAX *Smart Mater. Struct.* **12** 845–50
- Cao H, Reinhorn M and Soong T T 1998 Design of an active mass damper for a tall TV tower in Nanjing, China *Eng. Struct.* **20** 134–43
- Crawley E F 1994 Intelligent structures for aerospace: a technology overview and assessment *AIAA J.* **32** 1689–99
- Fujita T, Enomoto M, Arikabe T, Ogawa T, Murai N, Hashimoto Y, Hamaguchi H and Kitahara T 2001 Active microvibration control of precision manufacturing factories with smart structure using piezoelectric actuators *Proc. SPIE* **4330** 449–59
- Fujita T, Shimazaki M, Hatayama T, Arikabe T, Murai N, Aizawa S and Toyama K 2002 Active vibration control of buildings with smart structure using large scale piezoelectric actuators *Proc. 3rd World Conf. on Structural Control* vol 3 pp 323–9
- Fujita T, Tagawa Y, Kajiwara K, Yoshioka H, Takeshita A and Yasuda M 1993 Active 6-dof microvibration control system using piezoelectric actuators *Proc. SPIE* **2040** 514–28
- Ghanem R and Shinozuka M 1995 Structural system identification. I: theory *J. Eng. Mech.* **121** 255–64
- Hagood N W and Anderson E H 1992 Simultaneous sensing and actuation using piezoelectric materials *Proc. SPIE—Int. Soc. Opt. Eng.* **1543** 409–21
- Kamada T, Fujita T, Hatayama T, Arikabe T, Murai N, Aizawa S and Tohyama K 1997 Active vibration control of frame structures with smart structures using piezoelectric actuators (vibration control by control of bending moments of columns *Smart Mater. Struct.* **6** 448–56
- Kar I N, Seto K and Doi F 2000 Multimode vibration control of a flexible structure using H_∞ -based robust control *IEEE/ASME Trans. Mechatron.* **5** 23–31
- Lazarus K B and Crawley E F 1992 Multivariable high-authority control of plate-like active structures *Proc. 28th AIAA/ASME/ASCE/AHS Structural* part 2 pp 931–45
- Ljung L 1999 *System Identification: Theory for the User* 2nd edn (Englewood Cliffs, NJ: Prentice Hall)
- Manning W J, Plummer A R and Levesley M C 2000 Vibration control of a flexible beam with integrated actuators and sensors *Smart Mater. Struct.* **9** 932–9
- Rew K H, Han J H and Lee I 2002 Multi-modal vibration control using adaptive positive position feedback *J. Intell. Mater. Syst. Struct.* **13** 13–22
- Saunders W R, Cole D G and Robertshaw H H 1994 Experiments in piezostucture modal analysis for MIMO feedback control *Smart Mater. Struct.* **3** 210–8
- Scott R G, Brown M D and Levesley M 2001 Pole placement control of a smart vibrating beam *8th Int. Congr. on Sound and Vibration (Hong Kong)* pp 387–91
- Soong T T 1988 State of the art review: active structural control in civil engineering *Eng. Struct.* **10** 74–84
- Spencer B F Jr and Sain M K 1997 Controlling buildings: a new frontier in feedback *IEEE Control Syst. Mag. Emerging Technol.* **17** 19–35
- Valliappan S and Qi K 2001 Review of seismic vibration control using smart materials *Struct. Eng. Mech.* **11** 617–36
- 2002 MATLAB *System Identification Manual* www.Mathworks.com